

Efficient photovoltaic energy conversion in tetracene-C₆₀ based heterojunctions

Chih-Wei Chu, Yan Shao, Vishal Shrotriya, and Yang Yang^{a)}

Department of Materials Science and Engineering, University of California Los Angeles, Los Angeles, California 90095

(Received 2 February 2005; accepted 11 May 2005; published online 9 June 2005)

We report organic solar cells fabricated with small-molecule organic semiconductor tetracene/C₆₀ heterojunction as the photoactive layer. The external power conversion efficiency of the devices under AM 1.5 solar illumination at 100 mW/cm² (1 sun) is 2.3±0.5% with relatively high open-circuit voltage ($V_{oc}=0.58\pm0.06$ V) compared to most of the other small-molecular donor-acceptor (D-A) heterojunction solar cells reported so far. Using atomic force microscopy and x-ray diffraction we found that tetracene thin films consist of submicron-sized grains with rough surface and well defined molecular order. Therefore, using high mobility polycrystalline tetracene thin films for D-A heterojunction devices dramatically increases area of tetracene and C₆₀ interface for exciton diffusion to reduce the recombination. © 2005 American Institute of Physics.

[DOI: 10.1063/1.1946184]

Organic photovoltaic are currently the focus of intense research efforts in numerous academic and industrial research laboratories for their potential applications in low-cost and flexible electronics.¹⁻³ Great progress has been made in solar cells based on interpenetrating polymer networks^{4,5} and dye-sensitized devices,⁶ showing that organic materials are suitable candidates for photovoltaics. Further, it has been demonstrated by Tang *et al.*¹ that the performance of the photovoltaic devices based on small molecules can be effectively enhanced by the donor-acceptor (D-A) heterojunction. More recently, Xue *et al.*³ demonstrated 4.2% power efficiency under intense simulated AM1.5G solar radiation based on the heterojunction between the electron donor copper phthalocyanine (CuPc) and the electron acceptor buckminsterfullerene (C₆₀). However, efficiencies of such devices are currently much lower than those of their inorganic counterparts, demanding further search for more efficient organic materials.

The low power conversion and quantum efficiencies of organic solar cells are mainly related to limited exciton diffusion to the charge separating interface as well as to poor carrier transport to the electrode. A prerequisite for efficient photon harvesting into electrical current is that the holes and electrons do not recombine before being swept out of the device to the external circuit. In order to reduce recombination, a donor material with high-hole mobility and an acceptor with high-electron mobility are ideal in the case of the D-A devices. Up until now CuPc are among the promising donor materials for organic solar cells. One material can also be use as donor material is the aromatic molecule tetracene, which has field effect mobility great than 0.1 cm²/V s and large photosensitivity.^{7,8} Moreover, the energy band gap of the tetracene is well suited for solar energy conversion. However, tetracene has received much attention as a promising material for organic thin-film transistors⁹ and Schottky-type photovoltaic cells,¹⁰ the photovoltaic with tetracene as donor materials has not been utility in organic heterojunction de-

vices. In this work we have investigated an efficient D-A photovoltaic cells based on a particular donor tetracene and well known acceptor C₆₀. A schematic diagram of a typical photovoltaic device employed and the molecule structure of the materials are shown in Fig. 1(a). Due to the polycrystalline tetracene has high mobility and suitable energy level associated with C₆₀ [Fig. 1(b)],^{11,12} the device shows large open-circuit voltage compared to most of small-molecular D-A heterojunction solar cells with high power conversion efficiency.

Organic donor/acceptor photovoltaic cells were constructed on patterned indium tin oxide (ITO)-coated glass substrates (10–20 Ω/sq sheet resistance) used as anode. After routine solvent cleaning, the substrates were treated with UV ozone for 15 min. The ITO substrate was then coated with a thin layer of the conducting polymer poly(3,4-ethylenedioxythiophene):poly(styrene sulfonate) (PEDOT:PSS) followed by drying at 120 °C for 15 min in ambient. The organic layers were grown by thermal evaporation with a background pressure of about 8×10⁻⁷ Torr. The organic materials used in the devices were tetracene (Sigma-Aldrich 97%) purified by thermal gradient sublimation prior to deposition, and C₆₀ (afla 99.5%) used as received. The tetracene layer of 800 Å was deposited at 0.2 Å/s over the anode followed by 300 Å of C₆₀ deposited at 1 Å/s. A 80 Å thick layer of bathocuproine (BCP) as an exciton blocking layer to complete the organic multilayers.¹³ Finally, a 1000 Å thick Al cathode was evaporated through shadow mask to define several devices with the active area of approximately 0.12 cm². All the electrical measurements were performed in a nitrogen-filled glove boxes at the room temperature. The current-voltage (*I-V*) curves were obtained by a Keithley 2400 source-measure unit. The photocurrent was measured under AM 1.5 solar illumination at 100 mW/cm² (1 sun) supplied by a ThermalOriel 150W solar simulator and light intensity has been monitored by calibrated silicon photodiode for a 1.5AM spectrum. Atomic force microscope (AFM) images were obtained using Digital Instruments Multimode Scanning Probe Microscope, operated in tapping mode, and x-ray diffraction were measured using Bede D1 system. The

^{a)} Author to whom correspondence should be addressed; electronic mail: yangy@ucla.edu

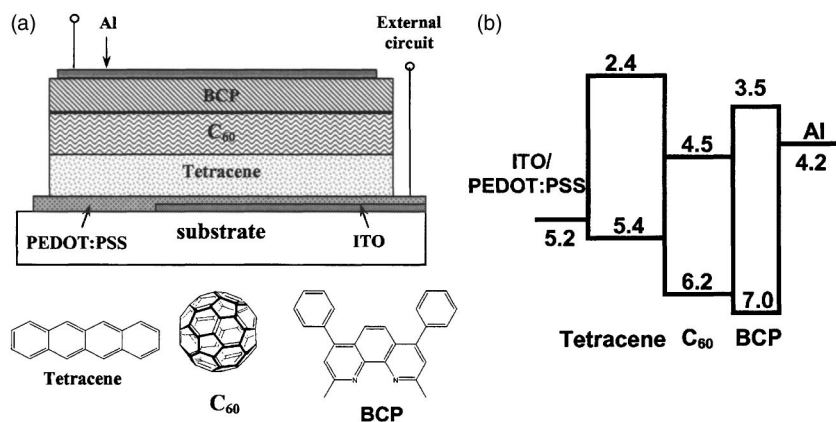


FIG. 1. (a) Schematic structure of the photovoltaic cells and chemical structures of organic materials (b) band diagram of a device.

absorption spectra were obtained from Varian Cary 50 UV-visible spectrophotometer.

Figure 2 shows dark and illuminated current density J -voltage (V) characteristics of the device with tetracene (800 Å) and C_{60} (300 Å) as the active layer. Under 100 mW/cm^2 AM1.5G illumination, the device shows an open-circuit voltage (V_{OC}) and a short-circuit current density (I_{SC}) of $0.58 \pm 0.06 \text{ V}$ and $7.0 \pm 0.5 \text{ mA/cm}^2$, respectively. The fill factor (FF), which is defined as $(V_{OC}^* I_{SC}) / (V_M^* I_M)$, was $57 \pm 5\%$. (V_M and I_M are the voltage and the current density at the maximum power output, respectively). These values give a photovoltaic conversion efficiency (defined by $\eta = V_{OC}^* I_{SC}^* \text{FF} / I_{PH}$, where I_{PH} is the incident photon flux) of $2.3 \pm 0.5\%$. From the figure, it was observed that in the first quadrant, the photocurrent was much higher than the dark current, and at a forward bias of 1.0 V the photocurrent density was about five times higher than the dark current density. The reason for this difference can be attributed to the phenomenon of photoenhanced current. Photoenhanced current has been observed in tetracene thin films earlier,¹⁴ when the sample was illuminated by light with wavelength in the single-exciton range, the current was much higher than the measured dark current.

Molecular ordering of tetracene film was examined by x-ray diffraction (XRD) scans with $\text{Cu } K\alpha$ radiation. The reported single-crystal structure of tetracene is triclinic.¹⁵ As

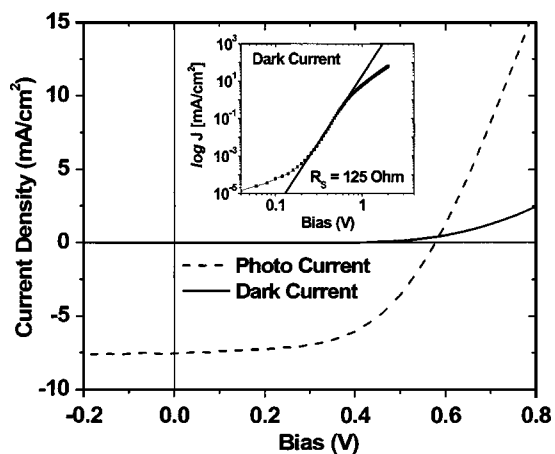


FIG. 2. Dark (solid line) and photo (dashed line) current density (J)-voltage (V) characteristics of a ITO/PEDOT/tetracene(80 nm)/ C_{60} (30 nm)/BCP(8nm)/Al device. The inset shows semilogarithmic scale J - V characteristics.

shown in Fig. 3, the XRD pattern for the tetracene film, with average thickness of 800 Å deposited at the rate of 0.2 Å/s onto a coated ITO substrate covered by PEDOT:PSS, exhibited a typical peak at $2\theta = 7.25^\circ$. From the literature¹⁶ this peak indicates that the film is c oriented with the long axis (c axis) of tetracene molecule oriented nearly perpendicular to the plane of the substrate and having an interplanar spacing of $d = 12.18 \pm 0.1 \text{ Å}$ that closely matches the expected (001) spacing of 12.26 Å for the single-crystal tetracene. Field effect transistor measurements revealed a hole mobility as high as $0.12 \text{ cm}^2/\text{V s}$ for well ordered tetracene films.¹⁶

Figure 4 is an AFM image of the topology of a tetracene film with an average thickness of 800 Å deposited at the rate of 0.2 Å/s onto a coated ITO substrate covered by PEDOT:PSS. This $5 \mu\text{m} \times 5 \mu\text{m}$ scan shows the film consists of numerous small grains approximately 300–500 nm in size with root-mean-square roughness of 9.7 nm. The film is very rough and we believe the voids between some grains extend to the substrate surface, resulting in irregular coverage by the film. The rough surface increases the area of the tetracene and C_{60} interface for better exciton dissociation. In contrast, it may cause some imperfections in the film and increase the contact resistance between Tetracene and C_{60} which results in the observed variations in the performance, especially for V_{OC} and FF. The series resistance of the photovoltaic device can be calculated from the $\log J$ - $\log V$ curves measured under dark. The series resistance is given as the offset from

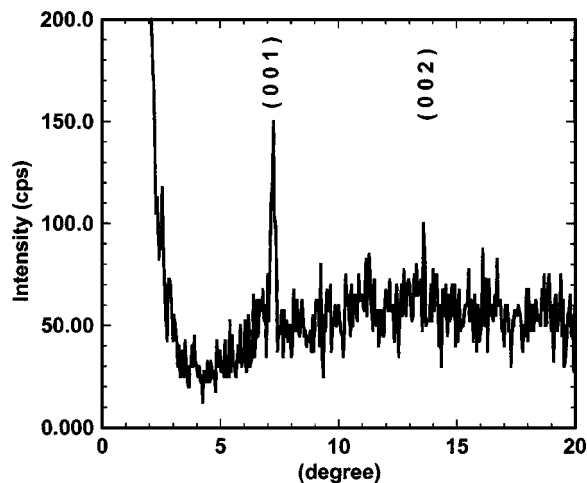


FIG. 3. XRD pattern for a tetracene film with an average thickness of 800 Å deposited on a coated ITO substrate cover by PEDOT:PSS.

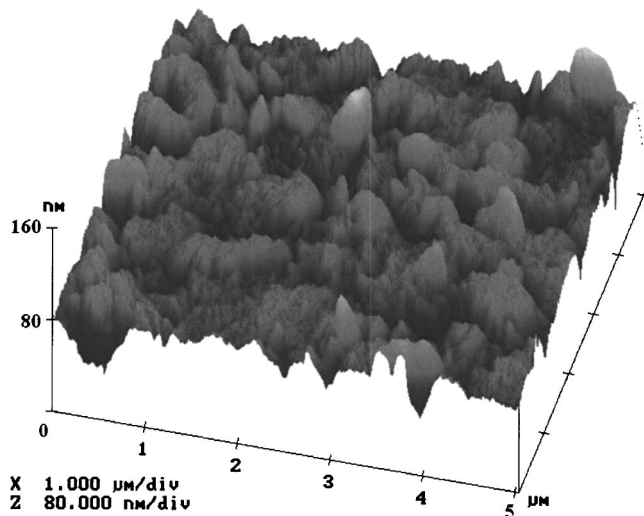


FIG. 4. $5\ \mu\text{m} \times 5\ \mu\text{m}$ atomic force microscope of a tetracene film with an average film thickness of $800\ \text{\AA}$ deposited on a coated ITO substrate cover by PEDOT:PSS.

linearity of the log I -log V curve at higher bias, $R_S = \Delta V / I$. From the dark I - V characteristics, we calculated the series resistance of the device to be $\sim 15\ \Omega$. The resistance of the device was slightly on the higher side than desired primarily because of the large thickness of the active layer and due to the large roughness of the tetracene/ C_{60} interface. Even though the resistance was high, a high FF was still obtained for the device. Therefore, by improving the morphology of the film, the resistance value can be further reduced to give even better FF. In order to improve the performance of these devices, further studies on improving the morphology are necessary.

Figure 5 shows the absorption spectra of tetracene and C_{60} , as well as tetracene/ C_{60} . The spectrum of tetracene shows a peak absorption near the middle of the visible spectrum with an absorption peak at $\lambda_{\text{max}} = 520\ \text{nm}$ and an absorption edge at $580\ \text{nm}$. On the other hand, C_{60} contributes a significant absorption in the short-wavelength range with an absorption maximum at $\lambda_{\text{max}} = 440\ \text{nm}$. Although the absorption spectra of tetracene and C_{60} films overlap in the short-wavelength range, both the tetracene and the C_{60} layers contribute to the photogeneration of the carriers and show complementary absorption spectra in the visible range.

In conclusion, the present results demonstrate that respectable photovoltaic performance can be achieved in a simple D-A structure based on polycrystalline tetracene and C_{60} . The substantial open-circuit voltage and photocurrent are attributed to the energy level of tetracene associated with C_{60} and the large exciton diffusion length of the high mobility polycrystalline tetracene thin film, respectively. Further

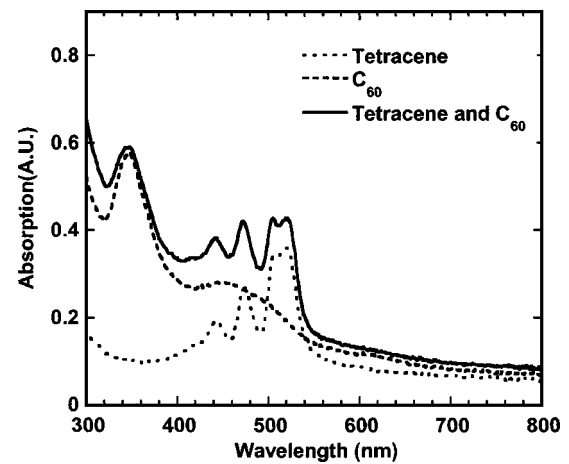


FIG. 5. Absorption spectra of tetracene, buckminsterfullerene (C_{60}), and tetracene/ C_{60} heterojunction.

improvements might be provided by optimizing growth rate of thin film and film thickness. Therefore, the demonstrated use of tetracene/ C_{60} heterojunction holds the promise of efficient low cost, large area “plastic solar cells.”

The authors would like to thank Y. T. Yeh for assistance with the XRD diffraction measurements. The financial support is provided by the Office of Naval Research, Program Manager Dr. Paul Armistead, Fund No. N00014-04-1-0403.

¹C. W. Tang, Appl. Phys. Lett. **48**, 183 (1986).

²G. Yu, J. Gao, J. C. Hummelen, F. Wudl, and A. J. Heeger, Science **290**, 1789, (1995).

³J. Xue, S. Uchida, B. P. Rand, and S. R. Forrest, Appl. Phys. Lett. **84**, 3012 (2004)

⁴S. E. Shaheen, C. J. Brabec, N. S. Sariciftci, F. Padinger, T. Fromherz, and J. C. Hummelen, Appl. Phys. Lett. **78**, 841 (2001)

⁵M. Granstrom, K. Petritsch, A. C. Arias, A. Lx, M. R. Andersson, and R. H. Friend, Nature (London) **395**, 257, (1998).

⁶U. Bach, D. Lupo, P. Comte, J. E. Moser, F. Weissörtel, J. Salbeck, H. Spreitzer, and M. Grätzel, Nature (London) **395**, 583, (1998).

⁷D. J. Gundlach, L. Zhou, J. A. Nichols, J.-R. Huang, and T. J. Jackson, Proc. IEEE **34**, 743 (2001).

⁸R. Signerski and J. Kalinowski, Thin Solid Films, **121**, 175 (1984).

⁹D. J. Gundlach, J. A. Nichols, L. Zhou, and T. N. Jackson, Appl. Phys. Lett. **80**, 2925 (2002).

¹⁰R. Signerski, G. Jarosz, and J. Godlewski, Macromol. Symp. **212**, 357, (2004).

¹¹M. Pope and C. Swenberg, *Electronic Process in Organic Crystals and Polymers*, 2nd ed. (Oxford University Press, New York, 1999).

¹²P. Peumans and S. R. Forrest, Appl. Phys. Lett. **79**, 126 (2001).

¹³P. Peumans, V. Bulovic, and S. R. Forrest, Appl. Phys. Lett. **76**, 2650 (2000).

¹⁴G. Jarosz, R. Signerski, and J. Godlewski, IEEE Trans. Dielectr. Electr. Insul. **8**, 422 (2001).

¹⁵R. B. Campbell, J. M. Robertson, and J. Trotter, Acta Crystallogr **15**, 289 (1998).

¹⁶D. J. Gundlach, J. A. Nichols, L. Zhou, and T. N. Jackson, Appl. Phys. Lett. **80**, 2925 (2002).